Aerosol Science and Technology

ISSN: 0278-6826 (Print) 1521-7388 (Online) Journal homepage: https://www.tandfonline.com/loi/uast20

Application of a FIGAERO ToF CIMS for on-line characterization of real-world fresh and aged particle emissions from buses

M. Le Breton, M. Psichoudaki, M. Hallquist, Å. K. Watne, A. Lutz & Å. M. Hallquist

To cite this article: M. Le Breton, M. Psichoudaki, M. Hallquist, Å. K. Watne, A. Lutz & Å. M. Hallquist (2019) Application of a FIGAERO ToF CIMS for on-line characterization of real-world fresh and aged particle emissions from buses, Aerosol Science and Technology, 53:3, 244-259, DOI: 10.1080/02786826.2019.1566592

To link to this article: https://doi.org/10.1080/02786826.2019.1566592

AEROSOL SCIENCE AND TECHNOLOGY
2019, VOL. 53, NO. 3, 244–259
https://doi.org/10.1080/02786826.2019.1566592

Application of a FIGAERO ToF CIMS for on-line characterization of real-world fresh and aged particle emissions from buses

M. Le Breton[a], M. Psichoudaki[a], M. Hallquist[a], Å. K. Watne[a], A. Lutz[a], and Å. M. Hallquist[b]

[a]Department of Chemistry and Molecular Biology, Atmospheric Science, University of Gothenburg, Gothenburg, Sweden; [b]IVL Swedish Environmental Research Institute, Gothenburg, Sweden

ABSTRACT

On-line chemical characterization of real-world particle emissions from 13 transit buses was performed using a chemical ionization mass spectrometer (CIMS) equipped with a filter inlet for gases and aerosols (FIGAERO). In addition to the fresh emissions the emissions were artificially aged using a potential aerosol mass reactor (Go:PAM). The buses studied were running on different fuel types (diesel, compressed natural gas, and rapeseed methyl ester) and exhaust after-treatment systems (selective catalytic reduction (SCR), exhaust gas recirculation (EGR), and a three-way catalyst). When evaluating emissions from passing exhaust plumes using the FIGAERO ToF-CIMS, two technical features were highlighted from this work, the use of high mass calibrants and the factor enhancement method to be able to filter important compounds from mass spectra including hundreds of species. Here, acetate was used as the reagent ion to enable detection of highly oxygenated species in the exhaust particle emissions with potential high toxicity and/or secondary organic aerosol formation (SOA) potential. The acetate ionization scheme accounted for 4% to 46% of the total emitted particulate mass through identification of 61 species in the spectra. For aged emission the various fuel types provided overlapping species that could explain up to 19% of the aged emissions. This is hypothesized to come from the oxidation of engine lubrication oil, thus a common source for various fuels which was further supported by laboratory measurements. Specific markers from the SCR technology, such as urea oxidation products and further byproducts from hydrolysis were identified and attributed to reactions of isocyanic acid.

ARTICLE HISTORY
Received 5 June 2018
Accepted 13 November 2018

EDITOR
Matti Maricq

Introduction

Volatile organic compounds (VOCs) are emitted into the atmosphere from a vast range of sources, both anthropogenic and biogenic. Their oxidation and reduction in volatility can lead to the formation of secondary organic aerosols (SOA) (Hallquist et al. 2009). Generally, enhanced particulate air pollutions cause serious health problems (Pope and Dockery 2006) and adversely affect air quality (AQ) and influence the climate. Here, traffic-related combustion processes contribute significantly to both emissions of primary particles and VOCs that cause negative effect as illustrated by Ots et al. (2016), who reported that diesel emissions, a source of carcinogens (IARC 2012), can contribute up to 30% of SOA in large cities. Diesel emissions are primarily composed of soot, which is formed by incomplete combustion (Bockhorn 1994; Kittelson et al. 1998), and organic species, which originate from the fuel and additives such as lubrication oil. Recent studies have suggested that lubrication oil can dominate the primary organic aerosol mass loading (Dallman et al. 2014) and due to its composition of cycloalkanes and aromatic compounds, it can also contribute significantly to SOA formation (Robinson 2007; Lim and Ziemann 2009; Gentner et al. 2012). Several studies have pointed out the SOA potential from light duty gasoline vehicles (e.g., Gordon et al. 2014; Platt et al. 2017; Pieber et al. 2018) while the concern regarding heavy duty vehicles (HDVs) has mainly been their primary emissions.

CONTACT M. Hallquist hallq@chem.gu.se Department of Chemistry and Molecular Biology, Atmospheric Science, Gothenburg, Sweden.
Color versions of one or more of the figures in the article can be found online at www.tandfonline.com/uast.
Supplemental data for this article can be accessed on the publisher's website.

However, recently, using a chemical tracer method a case study revealed a significant contribution from SOA originating from HDVs (Brito et al. 2018).

The public transport demands using HDVs are expected to continue to increase over the coming decade owing to growing urbanization and population around large cities (United Nations 2018), increasing the need for ways to control and reduce emissions from such sources. To alleviate other challenges associated with increased transportation, such as depleting oil resources and increased greenhouse gas emissions, the European Union has introduced new legislation stipulating that 10% of conventional road fuels (gasoline and diesel) must be replaced by alternative fuels by 2020, such as biodiesel, CNG, and rapeseed methyl ester (RME). However, emissions associated with these new alternative fuels are relatively unknown.

Several exhaust after-treatment systems (ATSs) are available for HDVs which decrease particle number and mass concentrations and also nitrogen oxide (NO_x) (a highly prioritized pollutant from vehicle combustion engines) emissions. Diesel oxidation catalyst (DOC) and diesel particulate filter (DPF) have an active catalytic coating which reduces particle mass via oxidation, whereas selective catalytic reduction (SCR) converts NOx into nitrogen and water via reaction with ammonia, which is usually initially formed by thermal degradation of urea. Exhaust gas recirculation (EGR) is another ATS for reducing the NOx emissions, where a part of the exhaust gas is recirculated back to the cylinders in order to decrease the combustion temperature and the oxygen content which reduces the formation of NOx. Although these systems have a positive impact on their specific target particulates or gaseous compounds, they can negatively impact emissions of other species. For example, DOC and DPF have been shown to increase the sulfur content in the particles (Maricq et al. 2002; Arnold et al. 2012), whereas DOC and SCR have been shown to decrease the mass loading of organics, but not affect the concentration of soot from heavy duty diesel engines (Karjalainen et al. 2012). EGR has shown to increase the emission of soot which may be due to the decrease in oxygen content when a part of the exhaust is recirculated, favoring soot formation (Maricq 2007; Hallquist et al. 2013).

Overall, the chemical composition and yield of particulate emissions from vehicles depends on several varying factors; engine type, ATSs, fuel additives such as lubrication oil, operation conditions (i.e., engine speed and engine load) but also environmental conditions such as temperature (Maricq 2007; Kittelson et al. 2008). Many studies on particle emissions have been done in test-benches, or motor labs using advanced dilution technology to mimic atmospheric dispersion (see e.g., Collier et al. 2015). They are very suitable to investigate specific parameters or technologies. In addition to such detailed studies there has been a growing interest in emission measurements in real-traffic situations where fast response instrumentations have enabled characterization on an individual vehicle basis by catching passing plumes (Jayaratne et al. 2007; Hak et al. 2009; Hallquist et al. 2013) or by chasing a specific vehicle (e.g., Canagaratna et al. 2004; Pirjola 2016). One may from such studies get real fleet variability in addition to how emissions vary with emission standard (e.g., Euro standards), fuel, and abatement technology. With applications on fast response instruments for chemical characterization a new field of emission studies has evolved. Saarkoski et al. (2017) recently utilized a soot particle aerosol mass spectrometer to chemically characterize the emissions of vehicles operating with various fuels and ATSs. They found that, although mass loading of emissions varied for different Euro standards (categorization of acceptable limits for exhaust emissions of vehicles sold in the EU and EEA member states), the composition of particle phase hydrocarbons varied insignificantly. Even if limited applications to vehicle emissions, recent instrumental developments have enabled tools for simultaneous online gas and particle phase measurements at high time resolution by utilizing a chemical ionization mass spectrometer (CIMS) (Lopez-Hilfiker et al. 2014). Here the acetate ionization scheme (one of several key ionization schemes applied in the literature) is a sensitive approach for measuring semi-volatile organic compounds (SVOCs), particularly acids, owing to its relatively weak acidity, and therefore ability to abstract a proton from many ambiently present SVOCs (Roberts et al. 2010).

Another evolving topic is to use the concept of estimating potential aerosol mass (PAM) by applying small reactors that simulates atmospheric oxidation from several precursors, including motor exhausts (Cubison et al. 2011; Li et al. 2011; Bruns et al. 2015; Tkacik et al. 2017). Studies have shown that PAM reactors can oxidize air masses to an atmospheric equivalent level of a few days within relatively short residence times with respect to classical smog chamber experiments (Bruns et al. 2015). Watne et al. (2018) recently deployed an oxidation flow reactor to "age" the primary emissions and probe the potential effect of atmospheric oxidation to buses operating with different fuels and ATSs. Secondary particle formation

Table 1. Summary of top 20 EF_{FRESH} and EF_{AGED} of PM contributing species in RME_{HEV}, CNG, and diesel emissions. EF_{TOTAL} (in mg kg^{-1}) and EF_{CIMS} observed are also calculated.

	RME_{HEV}			CNG			Diesel	
Species	EF_{FRESH} mg kg^{-1}	EF_{AGED} mg kg^{-1}	Species	EF_{FRESH} mg kg^{-1}	EF_{AGED} mg kg^{-1}	Species	EF_{FRESH} mg kg^{-1}	EF_{AGED} mg kg^{-1}
HNO_3[a]	1.200	35.000	HNO_3[a]	2.300	23.000	H_2SO_4[a]	3.400	2.600
$C_{18}H_{34}O_2$[b]	0.420	0.265	H_2SO_4[a]	1.200	0.020	HNO_3[a]	2.500	32.000
H_2SO_4[a]	0.300	0.290	C_7H_8O[b,c]	0.900	3.200	C_7H_8O[b,c]	2.300	16.700
HNCO[c]	0.120	0.120	$C_6H_5NO_3$[a]	0.800	2.100	$C_7H_4O_7$[b]	1.400	2.300
$C_6H_5O_2$[c]	0.089	0.076	$C_7H_4O_7$[b]	0.500	1.700	C_6H_5O[c]	1.400	8.200
$C_{14}H_{28}O_2$[b]	0.086	0.065	C_6H_5O[c]	0.300	2.600	$C_7H_7NO_3$[c]	0.800	1.900
$C_6H_5NO_3$[a]	0.068	0.475	$C_3H_6O_3$[a]	0.018	55.000	$C_3H_6O_3$[a]	0.040	50.000
$C_7H_7NO_3$[c]	0.051	0.343	$C_2H_4O_3$[a]	0.002	32.000	$C_2H_4O_3$[a]	0.020	10.000
$H_6S_2O_6$[b]	0.030	2.000	$C_6H_5O_2$[c]	0.100	2.300	$C_6H_5NO_3$[a]	0.400	1.800
$C_{18}H_{36}O_2$[b]	0.025	0.016	$C_7H_7NO_3$[c]	0.100	0.800	HNCO[c]	0.120	0.120
$C_{16}H_{32}O_2$[b]	0.021	0.030	$C_9H_{14}O_6$[b]	0.100	1.200	$C_2H_6O_2$[a]	0.100	9.300
$C_5H_8O_4$[b]	0.020	0.700	$C_2H_6O_2$[a]	0.080	2.500	$C_6H_5O_2$[c]	0.100	2.800
$C_4H_6O_4$[a]	0.020	3.400	$C_5H_8O_4$[b]	0.040	1.200	$C_9H_{14}O_6$[b]	0.100	0.800
$C_{16}H_{30}O_2$[b]	0.018	0.010	$C_4H_8SO_5$[d]	0.040	1.640	$C_4H_6O_5$[a]	0.054	82.000
$C_{18}H_{30}O_2$[b]	0.017	0.010	$H_6S_2O_6$[b]	0.003	2.000	$C_3H_4O_4$[a]	0.050	67.000
$C_3H_6O_3$[a]	0.015	40.000	$C_4H_6O_5$[a]	0.002	126.000	$C_5H_8O_4$[b]	0.050	2.300
$C_2H_4O_3$[a]	0.015	20.000	$C_4H_6O_4$[a]	0.002	3.400	$C_2H_5N_3O_2$	0.004	0.004
$C_{18}H_{32}O_3$[b]	0.013	0.012	$C_7H_{12}O_5$[b]	0.001	1.200	$H_6S_2O_6$[b]	0.003	2.000
$C_{18}H_{28}O_2$[b]	0.013	0.005	$C_7H_{10}O_5$[b]	0.001	1.300	$C_4H_6O_4$[a]	0.002	5.400
$C_{18}H_{34}O_3$[b]	0.013	0.003	$C_3H_4O_4$[a]	0.000	45.300	$C_2H_2O_3$[a]	0.001	1.000
EF_{TOTAL}	34.1	1322.0	EF_{TOTAL}	14.2	2140.0	EF_{TOTAL}	355.4	2467.0
EF_{CIMS}	2.7	297.4	EF_{CIMS}	6.5	323.6	EF_{CIMS}	12.9	312.9
% CIMS	7.8	22.5	% CIMS	45.7	15.1	% CIMS	3.6	12.7

[a]Directly calibrated.
[b]Indirect calibration via fit to C8 carboxylic acid.
[c]Relative calibration to similar functional group direct calibration.
[d]Relative glycolic acid sulfate calibration.

was shown to increase the mass loading by a factor greater than 10 for 79% of the buses, highlighting the importance of accounting for secondary particle formation when studying vehicle emissions.

This study assesses the utilization and optimization of a Filter Inlet for Gas and AEROsols (FIGAERO) Time of Flights (ToF) CIMS for chemical characterization of particulate emissions from an in-use bus fleet running on diesel, CNG, or rapeseed methyl ester (RME). The newly designed Gothenburg potential aerosol mass (Go:PAM) reactor was utilized to simulate aging of the fresh emissions from the studied buses (Watne et al. 2018), thereby enabling characterization of the chemical composition of particles emitted before and after atmospheric oxidation.

Experimental

Measurement design

The chemical particle characterization of bus emissions was carried out as part of a study on fresh and oxidized emissions from in-use transit buses where the plumes from passing busses were sampled at the curbside for on-line determination of various emission characteristics (Watne et al. 2018). In short, the particle and gaseous emissions from individual passing vehicles were determined by measuring the concentration change in the ambient diluted exhaust plume compared to the concentrations before the passage and relative to the change in CO_2 concentration. By this method it is not necessary to measure absolute concentrations as the relation to CO_2 is assumed to be constant during dilution (Jayaratne et al. 2007, 2008; Hak et al. 2009). In total 29 in-use buses were analyzed for which CIMS data of the fresh and oxidized, i.e., aged, particulate exhaust emissions were available for 13 of these buses: three diesel, five CNG, and five RME (of which four were electrical hybrids, RME_{HEV}). The non-hybrid RME bus was excluded from the detailed analysis presented here as it was considered that one bus may not fully represent the characteristics of its bus class and would skew the results. A summary of the buses' technical characteristics can be found in the supplementary information (SI) (Table S1). Figure 1 displays a simplified schematic of the experimental setup for the emission measurement.

The measurements were performed at two bus depots whose staff provided and maintained the buses. Each bus passed the sampling site while accelerating from standstill to about 20 km h^{-1}. Prior to measurement, the buses were driven for some distance to ensure the engines were fully warmed up. Three accelerations were measured for each bus and setting (i.e., fresh and aged emissions) to acquire statistical

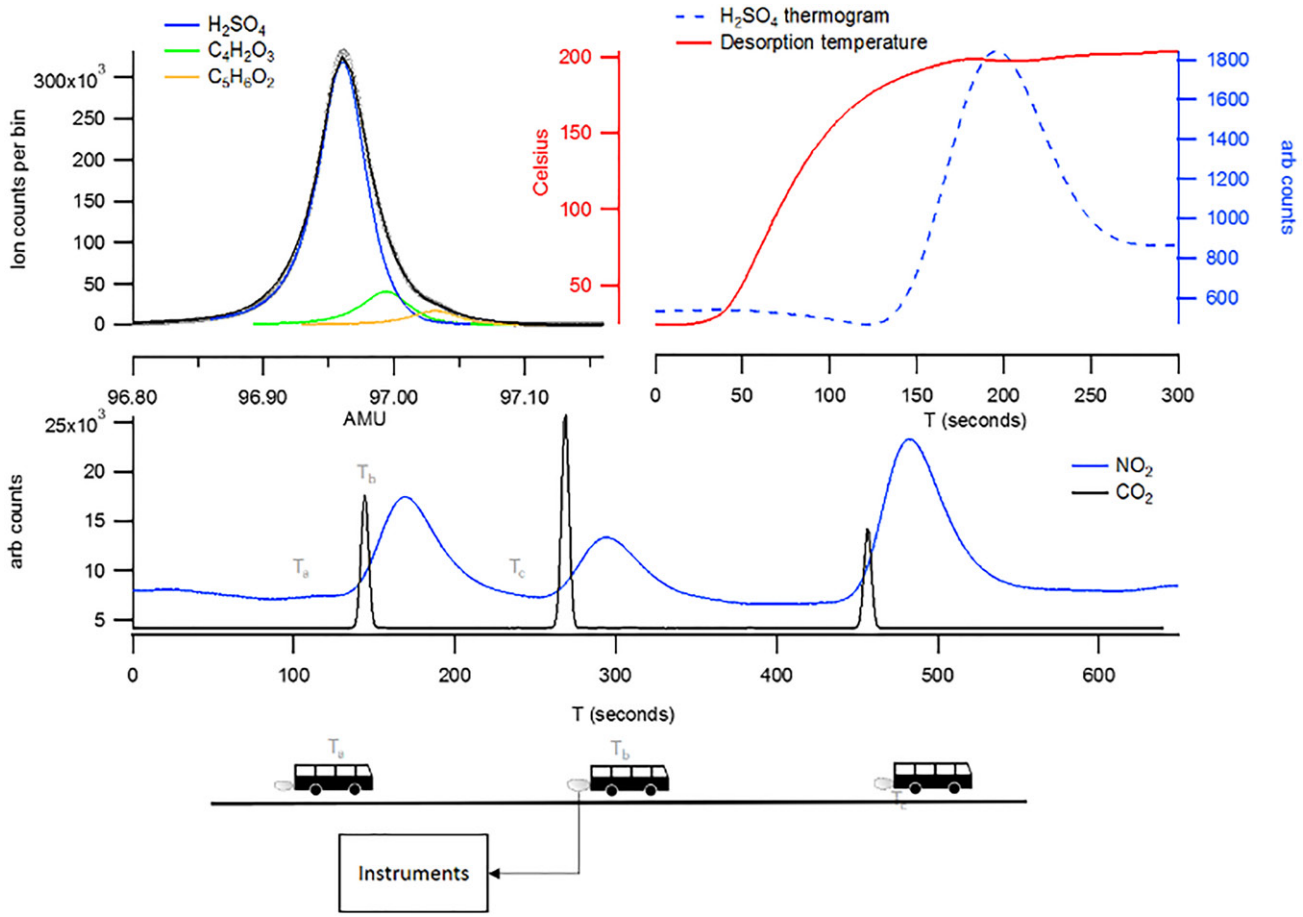

Figure 1. Representation of the experimental setup displaying the bus accelerating passed the inlets to the instruments (three times) to which gas phase and particle measurements are made. The middle panel displays these three passages of the bus as observed in elevated CO_2 and NO_2 concentrations. The top panels display the subsequent CIMS desorption profile for sulfuric acid (top right) and the corresponding high resolution peak fitting (top left).

significance. Supporting the CIMS analysis other particle and gas characteristics were also derived, all normalized to the integral CO_2 concentration of respectively plume measured using a non-dispersive infrared gas analyzer (LI-840A, LI-COR Inc.) at 1 Hz. Here an EEPS (engine exhaust particle sizer spectrometer, TSI Inc.) measured particle size distributions (both number and mass in the range of 5.6–560 nm) at 10 Hz (Hallquist et al. 2013) while gaseous NO, HC, and CO were measured by a remote sensing device (AccuScan RSD 3000, Environmental System Products Inc.) which was setup with a transmitter and receiver on one side of the passing lane and a reflector on the other, Burgard et al. (2006).

Oxidation

To evaluate the buses' potential for production of secondary particulate mass, an oxidation flow reactor (OFR) was utilized; the Gothenburg Potential Aerosol Mass Reactor (Go:PAM), which has previously been detailed by Watne et al. (2018). In principle, the Go:PAM exposes the extracted emission sample to a high concentration of hydroxyl radicals (OH) formed via the photolysis of ozone and subsequent reaction of water vapor. The Go:PAM consists of a 100 cm long, 9.6 cm i.d. flow reactor made of quartz glass (Raesh GmbH RQ 200) which can be illuminated by 2 Philips TUV 30 W fluorescent tubes, each radiating about 10 W at 254 nm, enclosed in a compartment with walls made from aluminum mirrors. The gas inside the reactor approaches laminar flow where a Reynold number <2000 is reached. The median reaction time was 35 s, providing sufficient oxidation of the air sample. The oxidation capacity of Go:PAM is estimated by calibrating with SO_2 as described by Kang et al. (2007) reaching an OH exposure of 5×10^{11} molecules cm^{-3} for sampling ambient air. This enables comparison of oxidation products and aerosol formation potential between various sources. The aged emissions are background corrected

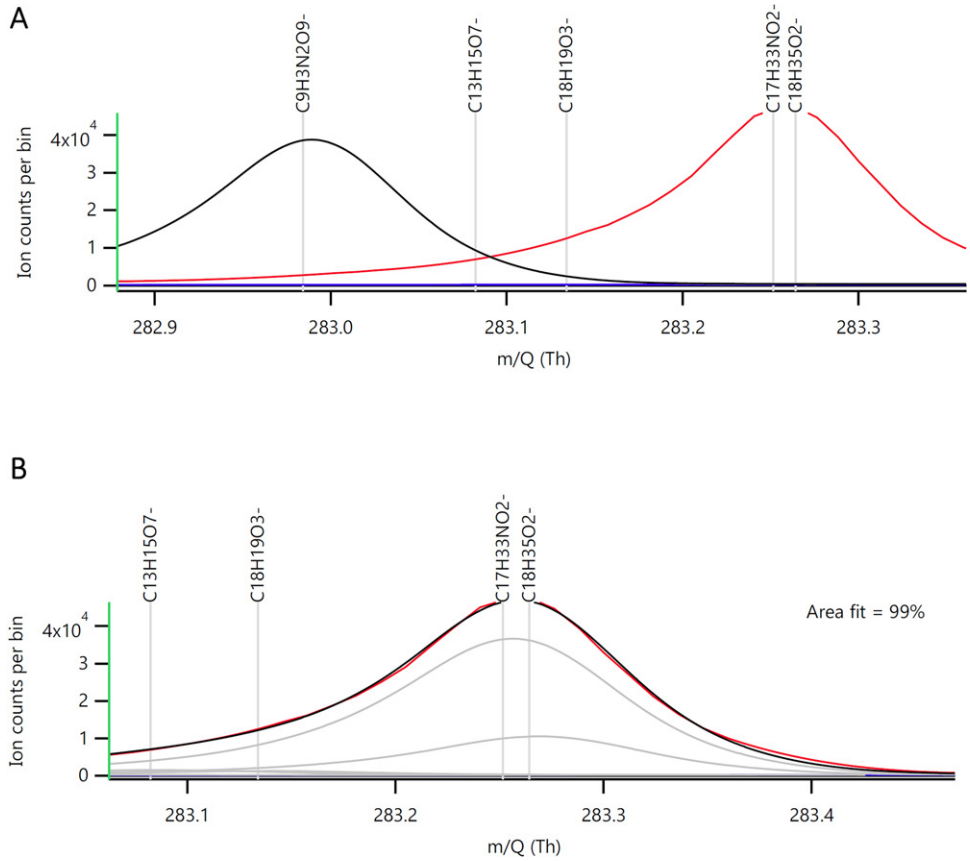

Figure 2. Average mass spectra for a bus desorption file focusing on the theoretical deprotonated mass for stearic acid ($C_{18}H_{36}O_2$). Plot A shows the theoretical mass peak at $m/z = 283.26$ and calibrated signal peak significant shifted to lower m/z (peak to the left) obtained by using standard mass calibrants. Plot B is the same plot but using PFPA as a mass calibrant and there is a perfect fit between theoretical and calibrated positions.

using data from oxidation of ambient air without bus-plume (measured with lamps on and no bus plume). This will thus account for the oxidation of background organics present in the system.

FIGAERO ToF-CIMS

A high resolution ToF-CIMS was utilized to measure semi-volatile species in the gas and particle phase of fresh and aged bus emissions. A detailed instrumental description can be found in previous literature (Bertram et al. 2011; Aljawhary, Lee, and Abbat 2013; Le Breton et al. 2017). Briefly, the instrument consisted of an ion-molecular reaction (IMR) chamber maintained at 100 mbar with a gas sampling flow of 2 standard liters per minute (SLM) where the species of interest are selectively ionized by acetate ions (particularly sensitive to more oxygenated organics) via proton abstraction, allowing negative ion detection in the ToF region. The acetate ions were formed by flowing 200 sccm N_2 (99.9% purity) over an acetic anhydride permeation source maintained at 50 °C, followed by dilution with 1.8 SLM N_2 (99.9% purity). This was then passed through an ion source (Po^{210} inline ionizer, NRD Inc, Static Solutions Limited), producing acetate ions as reagents.

Coupling of a FIGAERO to a ToF-CIMS has been described in detail previously (Lopez-Hilfiker et al. 2014). The dual inlet of the FIGAERO allows the gas sample flow (2 SLM) directly into the IMR for ionization of the gas phase components. During this period the second inlet provides a sample flow (2 SLM) thru a Teflon filter, collecting the particle phase. This filter can then be automated to move on a sliding arm enabling the particle phase to be evaporated into the IMR. The evaporation is facilitated by a heated dry nitrogen flow (2 SLM), thereby volatilizing the aerosol collected on the filter and enabling its detection in the IMR via gas phase reaction with the ionization ion.

In standard operation, the FIGAERO operates in a continuous cycle between gas and aerosol measurement to attain time series of particle and gas phase data. Typical operation of the FIGAERO comprises of 15 to 45 min sample/collection periods at a flow rate of 2 SLM. As previously described, each bus was sampled three times using the same method to obtain

consecutive collections onto the filter through a 3 meter long 10 mm OD copper tube, which should tripled the loading onto the filter. This result in a significantly lower collection time compared to the standard cyclic operation periods as each bus plume measured is around 1-min-long, but is compensated by a higher concentration in the bus plume compared to typical ambient sampling. The mass flow controller to the air flow over the filter was stopped between passages to reduce background mass to be collected onto the filter. After three bus passages (same bus individual), a N_2 flow over the filter was heated to 200 °C incrementally within 10 min and then maintained at that temperature for 5 min to ensure all mass was desorbed off the filter and reacted in the IMR of the mass spectrometer as gas phase molecules. The filter was replaced for each desorption to ensure replicability in relation to the background desorption, which was performed daily for both fresh and aged data.

Calibrations

The various chemical species measured in this work were quantified to obtain emission factors (EFs) from measured desorption count profiles via either direct calibration, if available, or an indirect method. Calibrations for carboxylic acids (C_1 to C_{10}), pyruvic acid, nitrophenol, and organic sulfates (OSs) are detailed in the SI. Standards were available for each of these compounds and were calibrated either using a permeation source for gas phase species, or doped onto the FIGAERO filter for solid state samples. For each species listed in Table 1 the calibration method (direct or type of indirect methods) are given and all applied sensitivities are found in the SI.

Mass calibration and peak identification

The instrument was initially set up to mass calibrate for known ions present throughout the measurement period, i.e., for species O_2^-, $HCOO^-$, NO_2^-, and $C_2H_3O_2^-$. However, initial peak identification analysis for the particulate data was inaccurate owing to large deviation in high mass identification due to skewing to lower masses for the mass calibrant peaks. Prior knowledge of bus emission data suggested that fatty acids (FA), such as oleic acid and stearic acid, should be emitted from RME fuels since they are comprised primarily from FAs. Indeed, the deprotonated mass of these acids was observed even in the low resolution 1 atomic mass unit (AMU) data, the so called stick data, representing integration of a whole mass unit without any baseline removal from the spectra, although high resolution (HR) analysis could not confirm the species to be these acids within an acceptable error. A solution was to utilize an injection of perfluoropentanoic acid (PFPA) where persistent peaks at 263, 526, and 720 Th were observed due to the high acidity and dimer/trimer formation. The HR data was recalibrated using the standard mass calibration species (mentioned above) and also PFPA with its corresponding dimer and trimer as reliable high mass calibrants, enabling accurate identification both of the low mass species and the high mass FAs (up to C_{27}) at 1 ppm accuracy. This was in contrast to the previously used calibrants, for which the peak was nearly 0.3 AMU lower than the calculated mass (Figure 2). Hence, in order to be able to detect high mass species in the emission from vehicles one must carefully utilize calibrants in the mass region of interest where e.g., perfluoropentanoic acid could be a good suggestion for future studies.

Desorption integral analysis

One known analytical limitation of the ToF-CIMS is quantification of all identifiable spectral peaks due to the varying affinity of the ionization source to different compounds resulting in sensitivities varying for all measured species. The acetate ion scheme is able to be highly sensitive to organic acids and oxygenated organics, as well as nitrated and sulfated organics, resulting in its ability to detect hundreds of species in the gas and particle phase. Currently it is implausible to calibrate for all species present in the spectra and to date; no method has been utilized to extrapolate a function of known parameters to constrain all sensitivities. Previous CIMS papers have applied sensitivities for specific species via direct calibration or assumed sensitivity for a functional group of compounds that the ionization of choice detects (Chhabra et al. 2015). The work presented here attempts to characterize fuel emissions containing a large suite of compounds which will have varying affinity to deprotonation by the acetate ion and therefore resulting in different sensitivities. Applying an appropriate sensitivity ensures that the dominant and key species emitted are prioritized appropriately. However, since the novel method here uses a plume capturing concept one may argue that any significant enhancement in signal could be used as traces/indicators for the emission. This relative increase compared to ambient concentrations would then be independent to the absolute

measured signal and its sensitivity. This further advances standard spectral analysis where one assuming the most intense peaks on the spectra to be of significant importance, as species such as formic acid and NO_3^- are very easily ionized by acetate but are likely to be in lower concentration than their intensity suggests. Sensitivity also decreases (in general) with an increase in molecular weight. A simple spectral subtraction value (SV) approach (subtracting a background spectrum from the plume spectrum) may not reveal important peaks at high masses, although we are likely to expect emissions from fuels to contain high mass organics that also could serve as good tracers in ambient air for a specific source.

For an initial analysis to determine species which increase relatively the most with respect to the background sampling, the integral of each desorption time series (the sum counts detected by the detector during the particle measurement cycle) was divided by the integral of the same mass from its respective background filter desorption. This allowed a factor enhancement (FE) value to be calculated for every identified mass peak relative to its background desorption for each bus. Figure S2 presents tables of the fresh emission results for bus ID_8 (RME fuel) ordered by either decreasing FE or the standard absolute subtracted value (SV). Only one of the top ten results occurs in both tables (highlighted in red), demonstrating that results may reflect either a real absolute concentration change or difference in sensitivity for different species. The table where peaks are ordered by decreasing SV is also dominated by ions known to be more prevalent in the gas phase and susceptible to reaction with acetate, whereas the FE method identified many heavier carboxylic acids, which are known to be present in high concentrations in RME fuels. It should be noted that this method does not fully overcome the sensitivity issue as when calculating EFs, a calibration factor is still necessary. It does however help to filter a large peak list to identify ions that change significantly relative to the background.

Emission factors

Emission factors for particle measurements assume that the CO_2 concentration is directly proportional to the fuel consumption assuming complete combustion. In the calculations, a C-fraction of 77.3%, 86.1%, and 69.2% was used for RME, diesel, and CNG, respectively (Edwards et al. 2014) to enable estimation of how much CO_2 would be produced by burning 1 kg of fuel assuming complete combustion. The reported EFs for the CIMS are in units of mg kg^{-1} of fuel burnt and were calculated for all PM contributing species from all measurements with either a high EF, derived by the standard SV method, or selected by having a significant FE (i.e., $>3\ \sigma$).

Results and discussion

Chemical characterization of fresh emissions

The diesel buses have the highest average $EF_{TOTAL:FRESH}$ (the emission factor for the total fresh particulate mass) observed using the engine exhaust particle sizer (EEPS) (355 ± 144 mg kg^{-1}) followed by the RME_{HEV} (34 ± 23 mg kg^{-1}) then CNG (14 ± 15 mg kg^{-1}), indicating that diesel is a significantly higher contributor to aerosol loading with respect to the newly developed alternative fuels. However, the diesel class included both Euro IV and Euro V buses, whereas the RME_{HEV} and CNG buses were Euro V or enhanced environmentally friendly vehicles (EEVs). In total, 61 condensed phase species were identified by CIMS as significant/relevant emissions from the different fuel types. The top 20 EF_{FRESH} are shown in Table 1, with respective EF_{AGED} (the full table can be found in the SI Table S2). The fresh diesel emissions measured by CIMS were dominated by HNO_3, H_2SO_4, and benzene oxidation products, with e.g., cresol having an EF_{FRESH} of 2.3 mg kg^{-1}. Nitrophenol and phenol also had relatively high EF_{FRESH} with 0.4 and 1.4 mg kg^{-1} respectively. CNG fresh emissions were dominated by H_2SO_4, representing 1.2 mg kg^{-1} of the total $EF_{CIMS:FRESH}$ (6.5 mg kg^{-1}). Relatively high EFs of oxidized/nitrated phenol products were also observed for CNG (EF_{Cresol} 0.9 mg kg^{-1} and $EF_{Nitrophenol}$ 0.8 mg kg^{-1}). The fresh RME_{HEV} emissions were comprised by a range of compounds from varying sources. FAs, specifically oleic acid (0.42 mg kg^{-1}), which is known to be a main component of the pre-burnt fuel (Usmanov et al. 2015) contributed significantly to the identified mass loading. Similarly to the other fuels, HNO_3 and H_2SO_4 were dominant compounds, but also, species related to the SCR technology and other organic acids were identified.

An interesting metric from an instrumental perspective is to compare the percentage mass observed by the CIMS for the different fuels in both fresh and aged exhaust plumes. The total EF_{CIMS} was significantly lower than that calculated by the EEPS (EF_{TOTAL}), although this is expected owing to the selectivity of the ionization scheme and inability to see metallic ions, soot and with low sensitivity for

some organic compounds (e.g., hydrocarbons). The CIMS accounted for 8%, 46%, and 4% of the RME_{HEV}, CNG and diesel $EF_{TOTAL:FRESH}$, respectively. The high sensitivity of the CIMS to H_2SO_4 and HNO_3 is likely to account for the high CIMS percentage observed for the CNG buses as they accounted for 25% of the total emissions. Both diesel and RME were quite poorly accounted for by CIMS in comparison to CNG, although this may be expected due to the expected low content of acids in the fuel exhaust. Functional groups such as ketones, alcohols, and aldehydes are not observed by CIMS, therefore we propose that the oxidation occurring within the combustion phase is likely to produce a higher proportion of organics with these functional groups, than with acid and di-acid groups.

Chemical characterization of aged emissions

Generally, the aged emission factors were an order of magnitude higher than the fresh (Watne et al. 2018). This illustrates the importance of accounting for potential secondary mass production when assessing the environmental impact of different fuel types. Although the fresh emission result may indicate a significant mass loading of diesel fuels, the aged data identifies how the CNG and RME_{HEV} fuels can produce significant high mass loadings once released into the atmosphere. The species from the CIMS aged measurements accounted for 23%, 15%, and 13% of aged RME_{HEV}, CNG and diesel EF_{TOTAL}. Although the CIMS is able to account for a significant increase in aged mass there is clearly a large amount of mass produced in the Go:PAM reactor which the ionization technique cannot detect.

The decrease of observed percentage mass by CIMS for CNG is likely to be caused by a similar reason, exacerbated by the high contribution of H_2SO_4 in the fresh emissions. This result indicates that oxidized mass is produced within the Go:PAM reactor that CIMS is able to detect, although there is significantly more mass made to which the instrument is blind to, indicating again that the acids may contribute to a relatively low fraction of the SOA. This agrees well with the AMS study by Tkacik et al. (2014) who suggest 10–22% of organics are formed during ageing. Even if the aged data in Tkacik et al. (2014) is mostly collected from petrol engines our results indicate that also diesel engines could produce a similar amount of SOA. On the contrary, Platt et al. (2017) conclude that petrol engines produce significantly more SOA than diesel. However, this comparison cannot be used directly since they analyze light duty vehicles and diesels with DPF. They also show how SOA from diesel fuels may only contain up to 4% acids and contains significant amount of carbonyls while our study has significantly higher contribution of organic acids.

Lubrication oil analysis

The RME_{HEV} EF_{AGED} were dominated by oxidized acids such as malonic, malic, succinic, and hydroxybutric acid. The CNG emissions showed a similar trend with many oxidized organics contributing to the aged emissions. Aged diesel emissions were dominated by similar acids as seen in RME_{HEV} and CNG and a number of nitrated organics and aromatics. Malic acid had the highest EF_{AGED} diesel value, 82 mg kg^{-1}, signifying a significant contribution to SOA from this source, but was also high in CNG and RME_{HEV}, relative to their EF_{TOTAL} (126 and 62 mg kg^{-1}, respectively).

The similar emission pattern where malic acid and other commonly emitted compounds were found for all fuels may not be an expected result. The significant mass contributing compounds are displayed in SI Table S3 and feature compounds such as malonic, malic, succinic, propionic acid, and H_2SO_4. These non-fuel dependent emissions which were present in all three fuel types contributed to 9% of $EF_{TOTAL:FRESH}$ for CNG, 1% for RME_{HEV}, and 1% for diesel. The aged emissions of these compounds represented a higher percentage on average of the $EF_{TOTAL:AGED}$ (19% for RME_{HEV}, 13% for CNG, and 9% for diesel), with the RME_{HEV} mass increasing by a factor of 112 for these 11 compounds. These compounds represent up to 28% of all EF_{FRESH} measurable by acetate CIMS and up to 84% of the EF_{AGED} indicating that oxidation of the fuel itself is either not an important SOA mass contributor or that the oxidation products of the fuel are not identifiable by the acetate CIMS. The different compositions of the fuels and ubiquitous signal of H_2SO_4 indicates a common source, specifically for the RME and CNG fuels, which were expected to contain very little H_2SO_4 as a contaminant (Pirjola et al. 2015). Durbin, Zhu, and Norbeck (2003) has shown that lubrication oil may contain up to 0.76% sulfur, supporting the theory that lubrication oil could be the common source. There are likely to be a much larger range of compounds which are unique to lubrication oil emissions from engines, such as C_{20}-C_{39} polycycloalkanes, which Eichler et al. (2017) illustrated is a dominant composition of lubrication oil in ship exhausts, paraffin from

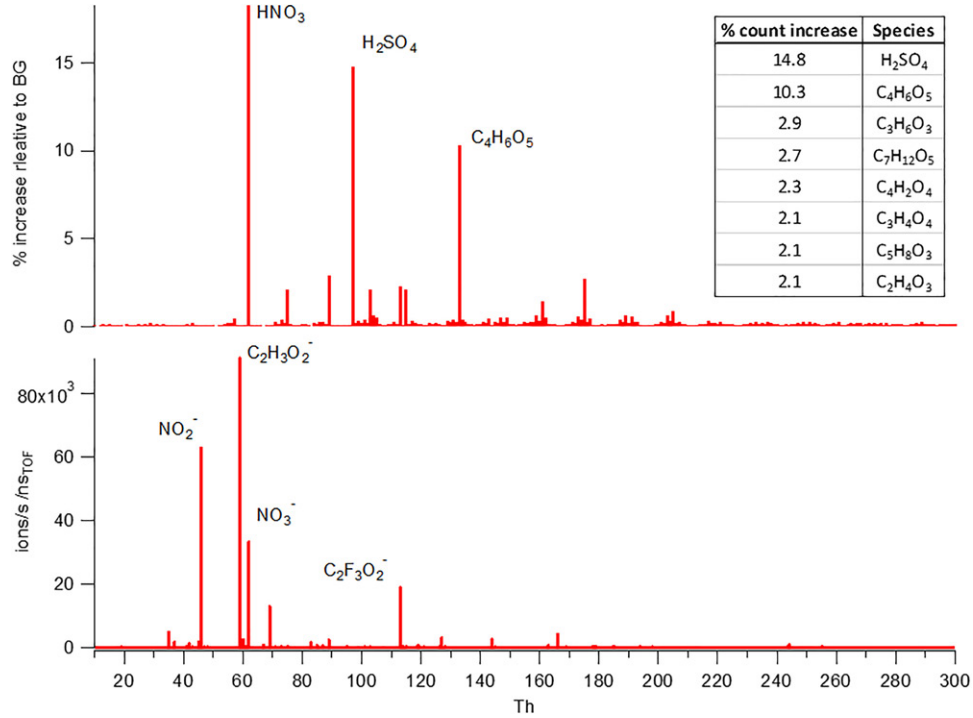

Figure 3. Illustrating of the CIMS results from measuring lubrication oil after being nebulized and passed through the Go:PAM reactor. The bottom panel shows the average Go:PAM background MS during desorption with no addition of lubrication oil and the top panel represents the % increase of signal for each mass during calibration. The top right table illustrates the species which increased the most relative to the background.

on-road vehicles highlighted by Dallmann et al. (2014) and metals such as zinc (Pirjola et al. 2015). Worton et al. (2014) also found that OC measured in a tunnel was dominated by lubrication oil. Therefore, we suggest that these acids are products of oxidation and fragmentation of the larger carbon chained molecules present in lubrication oil. To further investigate the source, lubrication oil utilized in the diesel buses was nebulized, aged through Go:PAM and subsequently measured by the FIGAERO. All species represented in SI Table S3 as non-fuel dependent products were observed within the spectra as major masses. Thirty-nine species detectable by CIMS contributed to a signal increase greater than 1% with HNO_3 and H_2SO_4 contributing to over a third of the signal. The spectral analysis and peaks of interest are presented in Figure 3. We omit HNO_3 signals from this calibration due to its likely high production from $OH + NO_2$, rather than from the lubrication oil itself. Lubrication oil may not be the sole source of these acids in the emissions, which is indicated by their presence (although at much lower levels) in the fresh emissions. Bock et al. (2017) show that gas phase dicarboxylic acids can be produced in diesel engines (via combustion) at low exhaust temperatures, although do not play a role in primary particle nucleation. The EF_{FRESH} for malonic and succinic acid here (0.05 and 0.002 mg kg^{-1}) are much lower than in Bock et al. (2017) (0.172 and 0.293 mg kg^{-1}, respectively), indicating a possibility that they are formed via oxidation of HCs from the fuel, although secondary formation of dicarboxylic acids is much more significant; likely as a result of lubrication oil oxidation.

Focused analysis of emission subcategories

Inorganic and organic sulfur emissions

H_2SO_4 had the highest mass loading for the diesel buses (3.4 mg kg^{-1} representing 26% of EF_{CIMS}) followed by CNG and RME_{HEV}. Analysis of the HSO_4^- signal for H_2SO_4 (due to H abstraction) often displayed a double peak profile during desorption, indicating the possible breakdown of other sulfur containing species during heating due to fragmentation or interference from another ion. Figure 4 shows both a standard H_2SO_4 desorption profile and an example of the double peak desorption profile. The desorption of another unrelated mass is also shown to exclude the possibility that there was a leak or an anomaly occurring across the whole mass range. Previous work focusing on organosulfates (OSs) has indicated that some OSs can dissociate, by proton extraction from the C_2 position, and form bisulfate

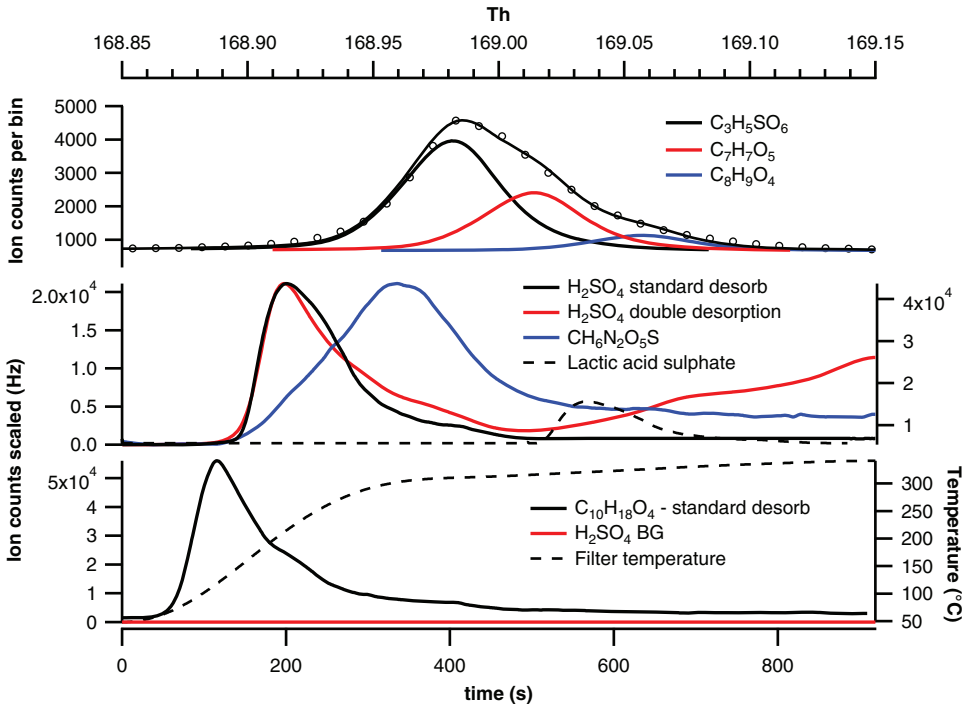

Figure 4. Peak fitting for lactic acid sulfate (LAS) ($C_3H_5SO_6$) and its subsequent desorption profile displayed with H_2SO_4 standard and nonstandard (with double desorption) profiles and urea sulfate ion. The $C_{10}H_{18}O_4$ desorption profile is displayed as a guideline for what a "standard" desorption by the FIGAERO produces.

depending on their structure. The bisulfate (mass 97 - HSO_4^-) can thus be used as a marker for OSs (Attygalle et al. 2001). Therefore, it is possible that the double desorption at the mass of HSO_4^- could be due to the release of HSO_4^- from dissociating OSs. Laboratory calibrations of glycolic acid sulfate (GAS) confirmed the production of HSO_4^- and H_2SO_4 for OSs (SI Figure S3). In those specific laboratory experiments the I^- ionization scheme was utilized since both ions and adducts can be formed during ionization. This allowed detection of both the HSO_4^- as an ion and H_2SO_4 as an I-adduct, because they exhibit different desorption profiles with respect to temperature during OS calibration.

Studies have shown that OSs can form ambiently in concentrations detectable by CIMS (Olson et al. 2011) and have recently been identified in diesel and biofuel SOA using offline high mass resolution techniques (Blair et al. 2018). Deprotonated masses of several possible OSs were identified, although it must be noted that not all represented the major peak within the spectral fit. In total, 11 potential OS peaks were identified with 2 ppm error during the identification process (so called peak list building process) which exhibited standard desorption profiles. The number of OSs identified here is limited to peak fitting and peak intensity and therefore may not represent the total budget of OSs formed, but rather a validation of their presence, supporting the work of Blair et al. (2018). An overlap of a number of these peaks identified between the two datasets further confirms the correct identification.

Diesel emissions had the highest EF_{AGED} (11 mg kg^{-1}) for OS mass followed by RME_{HEV} and then CNG (SI Figure S4). Aged diesel emissions contained significant levels of C_6-C_9 OSs, which we hypothesize are OSs from aromatic precursors, who are likely to be co-emitted with sulfur from the lubrication oil. Here a C_8 OS appears to contribute to a significant amount of OS mass for the diesel emissions, in line with Blair et al. (2018). RME_{HEV} also emitted C_6-C_8 OSs indicating the possible presence of benzene in the exhaust, possibly originating from natural contaminants in the fuel. The CIMS technique is blind to structure, so we cannot confirm that the C_6-C_8 OSs are aromatic or aliphatic.

The CNG OS composition is mostly dominated by lactic acid sulfate (LAS) and (GAS), which were also present in diesel and RME_{HEV}. Glyoxal is known to be formed by the oxidation of benzene (although has other sources) within the fuel with a yield of around 35% (Volkamer, Platt, and Wirtz 2001) and may therefore act as a precursor to GAS. If it is assumed that all glyoxal reacts with H_2SO_4 to form GAS, it can be estimated that 1.8 mg kg^{-1} was emitted from the CNG buses (assuming 0.7 mg of benzene was emitted

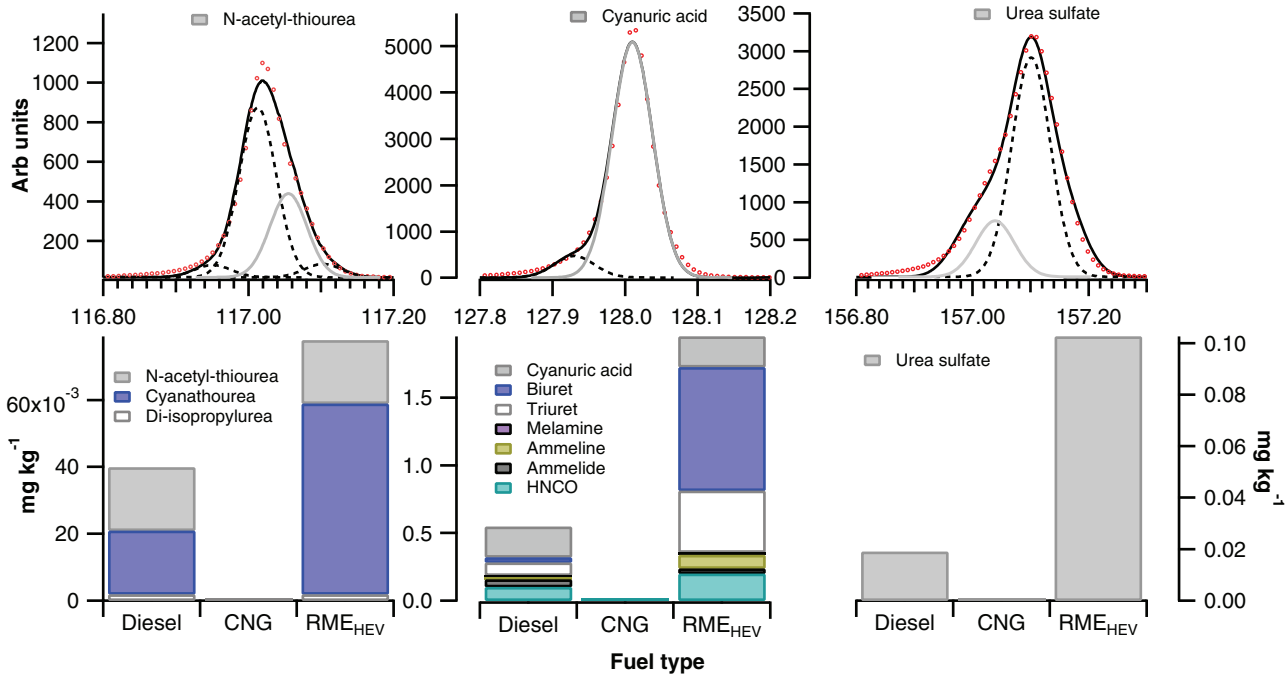

Figure 5. Urea oxidation products and further byproducts of isocyanic acid and salt formation. Spectral fits for key species are highlighted to illustrate the accuracy of identification.

per kilometer [Kelly, Bailey, and Coburn 1996]), agreeing relatively well with the 1.64 mg kg^{-1} EF for CNG buses calculated in this work.

SCR technology

The diesel and RME_{HEV} buses operated using SCR technology, converting NO_x into nitrogen and water via reaction with ammonia, formed via thermal degradation of urea. Isocyanic acid (HNCO) is also produced by the thermal degradation of urea but is then assumed to be efficiently hydrolyzed to form ammonia. During the desorption analysis, several urea related peaks were identified in the mass spectra of all RME_{HEV} and diesel buses, both types utilizing SCR technology as shown in Figure 5. Laboratory calibration using an AdBlue® (urea and water) liquid solution confirmed that these products could be detected after ageing in the Go:PAM reactor; providing a unique marker after atmospheric processing for buses utilizing SCR technology.

The EF_{AGED} values for the diesel bus urea oxidation products were a factor of two lower than those of the RME_{HEV} buses. This may be explained by the higher efficiency of the SCR technology in the diesel buses, which reduces NO_x more effectively (EF_{NOx} 15 ± 3 and 30 ± 12 g kg^{-1} for diesel and RME_{HEV}, respectively) and increases urea conversion to ammonia. This was also observed for the signal attributed to urea sulfate, where a significantly larger emission was observed for RME_{HEV} buses even though $EF_{H2SO4:FRESH}$ was ten times higher for diesel.

Gas phase measurements of HNCO indicated inefficient hydrolysis of HNCO, enabling HNCO to further react via several pathways, a known major problem of SCR technology (Bernhard et al. 2012; Wentzell et al. 2013). Upon initial analysis of the HNCO byproducts, the RME_{HEV} fuel appeared to emit more mass than the diesel buses, with biuret and triuret dominating, whereas the diesel emissions were composed mainly of cyanuric acid, HNCO and triuret. HNCO was a significant particle phase mass contributor for all SCR related peaks, which is unexpected due to its partitioning significantly to the gas phase. HNCO began to come off the filter at 84 °C and exhibited two maximum in desorption temperature (T_{max}) at 182 °C and 200 °C. The desorption profile did not return to background levels after the final T_{max} value and continued reporting a constant amount of counts after a small dip, suggesting a number of sources of HNCO from the filter. HNCO has a boiling point of 23.5 °C, therefore should begin to come off from the filter if present in the particle phase much earlier than observed. Urea has a melting point of 133 °C and vaporization starts around 140 °C. Upon vaporization it can decompose to form HNCO which can either further react with the remaining urea to form biuret or trimerise and form cyanuric acid. HNCO can further react with biuret to form ammelide and ammeline at temperatures up to

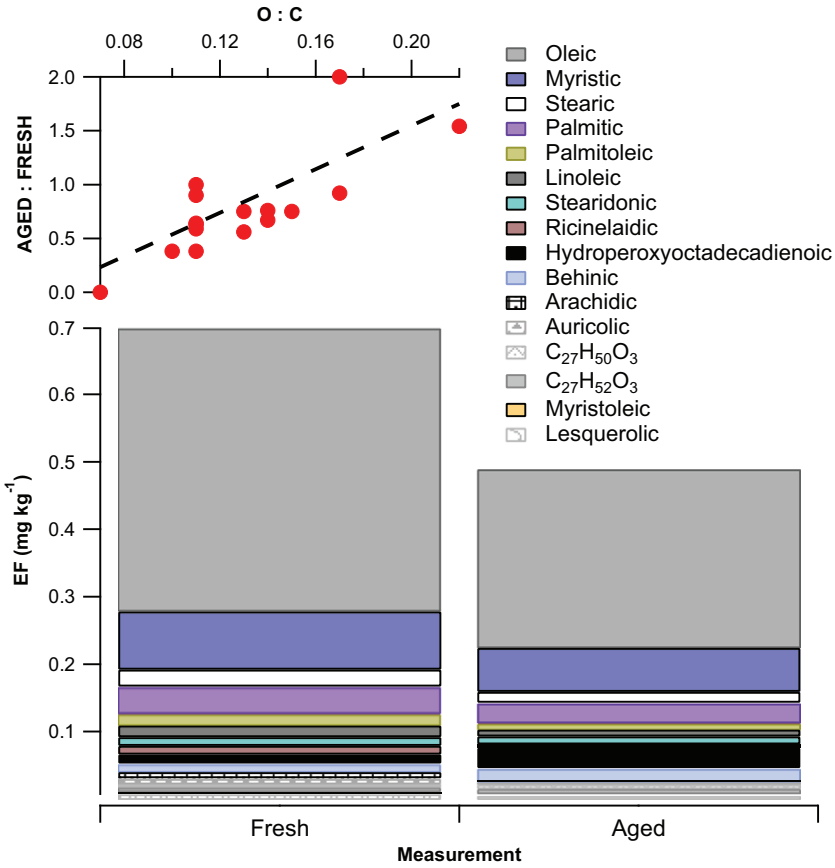

Figure 6. Contribution of FAs to the EF_{FRESH} and EF_{AGED} for RME_{HEV} buses. The top right panel illustrates the factor change of EF between EF_{FRESH} and EF_{AGED} as a function of O:C ratio of the FAs.

190 °C, with further reactions of biuret contributing to their production and cyanuric acid. At temperatures up to 250 °C, melamine can be formed via reaction of ammeline with ammonia. The ramping of temperature in the FIGAERO to 250 °C may add an unsolvable level of complexity due to the formation rates of a number of these compounds. A standard thermogram for these compounds is displayed in the supplementary (SI Figure S5) confirming the detection of these products, although production of HNCO complicates their direct quantification. We conclude that it is not possible to diagnose the exact composition of the emissions via analyzing relative desorption profiles observed by the CIMS. The high concentration of HNCO could simply be via consumption of byproducts to produce HNCO. Nevertheless, the ability for CIMS to identify these compounds enables the technique to positively confirm the production of these byproducts formed from incomplete hydrolysis of HNCO. Their detection by CIMS also confirms the emission of SCR system particle phase products into the urban atmosphere in forms other than urea and HNCO.

Fatty acid (FA) emissions

The FA emissions reported here agree well with Usmanov et al. (2015) with respect to the FA composition contribution, assuming that the FA emissions were the result of unburnt fuel. Oleic acid represented 1.2% of the FA fresh emissions and 0.02% of the aged FA emissions, with linoleic, palmitic, and stearic contributing a further 0.27% and 0.08% of the mass in the fresh and aged samples, respectively. The significant levels of oleic acid allowed the acid to be utilized as a marker for RME fuels. Measurement of FA ratios within the fuel could be utilized as an accurate method for identifying RME emissions within an air mass. This would depend highly on the initial fuel content, which may vary depending on the source of the fuel.

The fresh emissions of FAs for RME_{HEV} contributed 0.7 mg kg^{-1} of the EF_{CIMS} 2.7 mg kg^{-1} and EF_{TOTAL} 34 mg kg^{-1}, representing 2% of the total emissions (Figure 6). After aging through Go:PAM, the EF_{FAs} for RME_{HEV} decreased slightly to 0.5 mg kg^{-1}, although oleic acid remained the dominant FA emission. This shows a significant reduction in FA contribution to the total emitted mass, likely to result

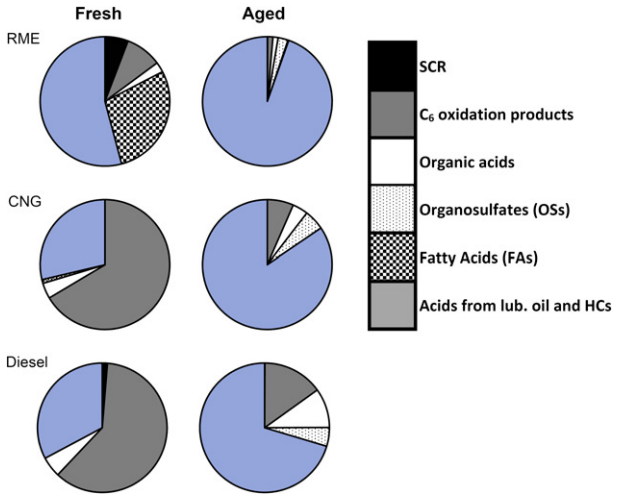

Figure 7. Mass composition measured by CIMS for the fuel types in fresh and aged emissions sorted into six source types: SCR technology, C_6 oxidation products, OSs, FAs, and acids which may come from multiple sources (FRESH – oxidation of lubrication oil during combustion and AGED – oxidation of lubrication oil, oxidation of fuel combustion species. Here the inorganic acids H_2SO_4 and HNO_3 were omitted.

from the increased contribution to aged mass from the engine or lubrication oil as postulated earlier and also further oxidation of FAs in Go:PAM. The engine combustion efficiency of an RME fuel is proportional to its composition with regards to degree of unsaturation (Hoekman et al. 2012). The results here show that the hybrid engines emission of FAs was oxidized to decrease its unsaturation content, which can be observed via a good correlation between the Aged:Fresh to O:C ratios (Figure 6).

Conclusions

The FIGAERO ToF CIMS utilizing the acetate ionization scheme was able to identify between 4 and 46% of the fresh and aged bus emissions of total particulate through identification of 61 unique species. This disperse range of coverage indicates the CIMS ability to probe chemical regimes and markers within fuel emissions, but it is also blind to many of the organics due to the high selectivity of the acetate ionization and inability to detect functional groups such as aldehydes and ketones. Its ability to simultaneously measure the particle and gas phase component of the emissions making its implementation unique in this field enabling the oxidation process forming SOA to be probed into further detail. To further enhance the use of the FIGAERO ToF CIMS, this work highlights two import technical features when evaluating emissions from passing exhaust plumes, the use of high mass calibrants, and the FE method.

The data analyzed here further supports that a non-fuel specific contribution to emissions, attributed to lubrication oil, may be important and therefore significant factor for future legislative considerations. The high concentration of H_2SO_4 observed indicates the necessity of regulating non-fuel-related additives, due to their apparent dominance of the SOA production and also significant contribution to primary mass. In addition to contributing to acidity, H_2SO_4 is a key compound in OSs formation, which are important secondary aerosol components (Le Breton et al. 2018) with respect to nanoparticle growth, and therefore CCN formation potential (Smith et al. 2008).

The emitted species related to the SCR technology can provide a useful insight into the efficiency of NO_x alleviation and impact on the catalyst. The observations of urea and its oxidation products highlight a significant source of HNCO and possible inefficient NO_x reduction process. Although the initial results suggest the unwanted byproducts from reactions of HNCO, predominantly cyanuric acid and biuret, are detectable by CIMS, their thermal dependency so far inhibits accurate analysis utilizing the FIGAERO. Nevertheless, their presence is observed and can support analysis of deposition to the catalyst, which results in a drop in NO_x conversion efficiency.

Fatty acid measurements provided important information from both an atmospherically relevant (SOA potential) and engine development perspective. The optimum composition, and therefore degree of saturation, of many fuels has not yet been determined, although this method of measurement provides vital information about the fuel content, fuel burn efficiency and how the emission content affects AQ owing to its composition and degree of unsaturation. The composition of the pre-burnt fuel was not available for the analysis, although independent testing could be utilized to compare the pre-burnt and emission content. This would enable optimization of the fuel content by reducing the FAs content within the fuel for the species that contribute a high proportion of the emissions as they are not oxidized within the engine.

An overall analysis of the emissions via CIMS measurement can be performed when considering the six sub categories of emission sources targeted in this work: lubrication oil, SCR technology, OSs, C_6 oxidation products, FAs, and other organic acids. Figure 7 displays the mass contribution of each of these sub categories for the three fuel types and for both fresh and aged measurements.

Overall, there is a clear dominance of lubrication oil related species for all fuels, which increases significantly when oxidized. C_6 oxidation products appear to be the second most prominent group in both CNG and diesel Fresh emissions. The CIMS is blind to structure and cannot differentiate between aliphatic and aromatic species, limiting the analysis of these compounds. Furthermore, higher mass aromatics and PAHs are likely to contribute to the emissions, not only C_6 oxidation products. Their absence here may be an indicator to a decreased sensitivity to these products, resulting in no identification in the spectra or not exceeding the 3 σ increase of FE above the background measurements. FAs are unique to RME_{HEV} and represent a significant mass fraction in the observed $CIMS_{FRESH}$ although are negligible in the $CIMS_{AGED}$. SCR related species are only found in measurable amounts in the RME_{FRESH} and $Diesel_{FRESH}$. Other organic acids and OSs are present but in relative insignificant levels compared to the FA and lubrication oil related species.

Acknowledgments

Support from Västtrafik, the organization responsible for public transport in all of Västra Götaland, Sweden, is gratefully acknowledged. The drivers and personnel at the measurement sites are also gratefully acknowledged for their assistance and hospitality.

Funding

This work was financed by Vinnova, Sweden's Innovation Agency (2013-03058) and the Swedish Research Council Formas (214-2013-1430).

References

Aljawhary, D., A. K. Y. Lee, and J. P. D. Abbat. 2013. High-resolution chemical ionization mass spectrometry (ToF-CIMS): Application to study SOA composition and processing. *Atmos. Meas. Technol.* 6(11):3211–24. doi: 10.5194/amt-6-3211-2013.

Arnold, F., L. Pirjola, T. Rönkkö, U. Reichl, H. Schlager, T. Lähde, J. Heikkilä, and J. Keskinen. 2012. First onLine measurements of sulfuric acid gas in modern heavy duty diesel engine exhaust: Implications for nanoparticle formation. *Environ. Sci. Technol.* 46(20):11227–34. doi: 10.1021/es302432s.

Attygalle, A. B., S. Garcia-Rubio, J. Ta, and J. Meinwald. 2001. Collisionally-induced dissociation mass spectra of organic sulphate anions. *J. Chem. Soc. Perk. T.* 2:498–506. doi: 10.1039/b009019k.

Bernhard, A. M., D. Peitz, M. Elsener, A. Wokaun, and O. Kröcher. 2012. Hydrolysis and thermolysis of urea and its decomposition byproducts biuret, cyanuric acid and melamine over anatase TiO2. *App. Cat. B: Environ.* 115–116 :129–37. doi: 10.1016/j.apcatb.2011.12.013.

Bertram, T. H., J. R. Kimmel, T. A. Crisp, O. S. Ryder, R. L. N. Yatavelli, J. A. Thornton, M. J. Cubison, M. Gonin, and D. R. Worsnop. 2011. A field-deployable, chemical ionization time-of-flight mass spectrometer. *Atmos. Meas. Technol.* 4 (7):1471–79. doi: 10.5194/amt-4-1471-2011.

Blair, S. L., A. C. MacMillan, G. T. Drozd, A. H. Goldstein, R. K. Chu, L. Paša-Tolić, J. B. Shaw, N. Tolić, P. Lin, J. Laskin, et al. 2017. Molecular characterization of organosulfur compounds in biodiesel and diesel fuel secondary organic aerosol. *Environ. Sci. Technol.* 51 (1):119–127. doi: 10.1021/acs.est.6b03304.

Bock, N., M. M. Baum, M. B. Anderson, A. Pesta, and W. F. Northrop. 2017. Dicarboxylic acid emissions from after treatment equipped diesel engines. *Environ. Sci. Technol.* 51 (21):13036–43.

Bockhorn, H. 1994. *Soot formation in combustion*. Vol. 59 of *Springer series in chemical physics*. Berlin, Heidelberg: Springer. doi:10.1007/978-3-642-85167-4.

Brito, J., S. Carbone, D. A. Monteiro dos Santos, P. Dominutti, N. de Oliveira Alves, L. V. Rizzo, and P. Artaxo. 2018. Disentangling vehicular emission impact on urban air pollution using ethanol as a tracer. *Sci. Rep.* 8: 10679.

Bruns, E. A., I. El Haddad, A. Keller, F. Klein, N. K. Kumar, S. M. Pieber, J. C. Corbin, J. G. Slowik, W. H. Brune, U. Baltensperger, et al. 2015. Inter-comparison of laboratory smog chamber and flow reactor systems on organic aerosol yield and composition. *Atmos. Meas. Technol.* 8 (6):2315–32. doi: 10.5194/amt-8-2315-2015.

Burgard, D. A., G. A. Bishop, R. S. Stadtmuller, T. R. Dalton, and D. H. Stedman. 2006. Spectroscopy applied to on-road mobile source emissions. *Appl. Spectrosc.* 60 (5):135A–48A.

Canagaratna, M. R., J. T. Jayne, D. A. Ghertner, S. Herndon, Q. Shi, J. L. Jimenez, P. J. Silva, P. Williams, T. Lanni, F. Drewnick, et al. 2004. Chase studies of particulate emissions from in-use New York city vehicles. *Aerosol Sci. Technol.* 38 (6):555–73. doi: 10.1080/02786820490465504.

Chhabra, P. S., A. T. Lambe, M. R. Canagaratna, H. Stark, J. T. Jayne, T. B. Onasch, P. Davidovits, J. R. Kimmel, and D. R. Worsnop. 2015. Application of high-resolution time-of-flight chemical ionization mass spectrometry measurements to estimate volatility distributions of a-pinene and naphthalene oxidation products. *Atmos. Meas. Technol.* 8 (1):1–18. doi: 10.5194/amt-8-1-2015.

Collier, S., S. Zhou, T. Kuwayama, S. Forestieri, J. Brady, M. Zhang, M. Kleeman, C. Cappa, T. Bertram, and Q. Zhang. 2015. Organic PM emissions from vehicles: Composition, O/C ratio, and dependence on PM concentration. *Aerosol Sci. Technol.* 49 (2):86–97. doi: 10.1080/02786826.2014.1003364.

Cubison, M. A., A. M. Ortega, P. L. Hayes, D. K. Farmer, D. Day, M. J. Lechner, W. H. Brune, E. Apel, G. S. Diskin, J. A. Fisher, et al. 2011. Effects of aging on organic aerosol from open biomass burning smoke in aircraft and laboratory studies. *Atmos. Chem. Phys.* 11 (23): 12049–64. doi: 10.5194/acp-11-12049-2011.

Dallmann, T. R., T. B. Onasch, T. W. Kirchstetter, D. R. Worton, E. C. Fortner, S. C. Herndon, E. C. Wood, J. P. Franklin, D. R. Worsnop, A. H. Goldstein, et al. 2014. Characterization of particulate matter emissions from on-road gasoline and diesel vehicles using a soot particle aerosol mass spectrometer. *Atmos. Chem. Phys*. 14 (14): 7585–99. doi: 10.5194/acp-14-7585-2014.

Durbin, T. D., X. Zhu, and J. M. Norbeck. 2003. The effects of diesel particulate filters and a low-aromatic low-sulfur diesel fuel on emissions for medium-duty diesel trucks. *Atmos. Environ*. 37(15):2105–16. doi: 10.1016/S1352-2310(03)00088-8.

Edwards, R., J.-F. Larive, D. Rickeard, and W. Weindorf. 2014. Well-to-wheels analysis of future automotive fuels and powertrains in the European context. JRC Technical Reports. Report EUR 26237 EN, V4a, Appendix 1. doi: 10.2790/95629.

Eichler, P., M. Muller, C. Rohmann, B. Stengel, J. Orasche, R. Zimmermann, and A. Wisthaler. 2017. Lubricating oil as a major constituent of ship exhaust particles. *Environ. Sci. Technol. Lett*. 4 (2):54–58. doi: 10.1021/acs.estlett.6b00488.

Gentner, D. R., G. Isaacman, D. R. Worton, A. W. Chan, T. R. Dallmann, L. Davis, S. Liu, D. A. Day, L. M. Russell, K. R. Wilson, et al. 2012. Elucidating secondary organic aerosol from diesel and gasoline vehicles through detailed characterization of organic carbon emissions. *Proc. Natl. Acad. Sci. USA* 109 (45):18318–23. doi: 10.1073/pnas.1212272109.

Gordon, T. D., A. A. Presto, A. A. May, N. T. Nguyen, E. M. Lipsky, N. M. Donahue, A. Gutierrez, M. Zhang, C. Maddox, P. Rieger, et al. 2014. Secondary organic aerosol formation exceeds primary particulate matter emissions for light-duty gasoline vehicles. *Atmos. Chem. Phys*. 14 (9):4661–78. doi: 10.5194/acp-14-4661-2014.

Hak, C. S., M. Hallquist, E. Ljungstrom, M. Svane, and J. B. C. Pettersson. 2009. A new approach to in-situ determination of roadside particle emission factors of individual vehicles under conventional driving conditions. *Atmos. Environ*. 43 (15):2481–88. doi: 10.1016/j.atmosenv.2009.01.041.

Hallquist, M., J. C. Wenger, U. Baltensperger, Y. Rudich, D. Simpson, M. Claeys, J. Dommen, N. M. Donahue, C. George, A. H. Goldstein, et al. 2009. The formation, properties and impact of secondary organic aerosol: Current and emerging issues. *Atmos. Chem. Phys*. 9 (14): 5155–236. 2009. doi: 10.5194/acp-9-5155-.

Hallquist, Å. M., M. Jerksjö, H. Fallgren, J. Westerlund, and Å. Sjödin. 2013. Particle and gaseous emissions from individual diesel and CNG buses. *Atmos. Chem. Phys*. 13 (10):5337–50. doi: 10.5194/acp-13-5337-2013.

Hoekman, S. K., A. Broch, C. Robbins, E. Ceniceros, and M. Natarajan. 2012. Review of biodiesel composition, properties, and specifications. *Renew. Sustain. Energy Rev*. 16 (1):143–69. doi: 10.1016/j.rser.2011.07.143.

IARC 2012. Diesel engine exhaust carcinogenic, International Agency for Research on Cancer, WHO, Press release N°213. https://www.iarc.fr/wp-content/uploads/2018/07/pr213_E.pdf.

Jayaratne, E. R., L. Morawska, Z. D. Ristovski, and C. He. 2007. Rapid identification of high particle number emitting on-road vehicles and its application to a large fleet of diesel buses. *Environ. Sci. Technol*. 41 (14):5022–27. doi: 10.1021/es063020v.

Jayaratne, E. R., C. He, Z. D. Ristovski, L. Morawska, and G. R. Johnson. 2008. A comparative investigation of ultrafine particle number and mass emissions from a fleet of on-road diesel and CNG buses. *Environ. Sci. Technol*. 42 (17):6736–42. doi: 10.1021/es800394x.

Kang, E., M. J. Root, D. W.Toohey, and W. H. Brune. 2007. Introducing the concept of Potential Aerosol Mass (PAM). *Atmos. Chem. Phys*. 7 (22):5727–44.

Karjalainen, P., T. R€Onkk€O, T. L€Ahde, A. Rostedt, J. Keskinen, S. Saarikoski, M. Aurela, R. Hillamo, A. Malinen, L. Pirjola, et al. 2012. Reduction of heavy-duty diesel exhaust particle number and mass at low exhaust temperature driving by the DOC and the SCR. *SAE Int. J. Fuels Lubr*. 5:1114–22. doi: 10.4271/2012-01-1664.

Kelly, K. J., B. K. Bailey, and T. C. Coburn. 1996. Round 1 emissions results from compressed natural gas vans and gasoline controls operating in the U.S. federal fleet. Presented at Society for Automotive Engineers International Spring Fuels and Lubricants Meeting, Dearborn, MI, May 6–8.

Kittelson, D. B., W. F. Watts, J. P. Johnson, C. Thorne, C. Higham, J. Payne, S. Goodier, C. Warrens, H. Preston, U. Zink, et al. 2008. Effect of fuel and lube oil sulfur on the performance of a diesel exhaust gas continuously regenerating trap. *Environ. Sci. Technol*. 42 (24):9276–82. doi: 10.1021/es703270j.

Le Breton, M., Y. Wang, Å. M. Hallquist, R. K. Pathak, J. Zheng, Y. Yang, D. Shang, M. Glasius, T. J. Bannan, Q. Liu, et al. 2017. Online gas and particle phase measurements of organosulfates, organosulfonates and nitrooxyorganosulfates in Beijing utilizing a FIGAERO ToF-CIMS. *Atmos. Chem. Phys. Disc*. 1–32.

Li, R., B. B. Palm, A. Borbon, M. Graus, C. Warneke, A. M. Ortega, D. A. Day, W. H. Brune, J. L. Jimenez, and J. A. de Gouw. 2013. Laboratory studies on secondary organic aerosol formation from crude oil vapors. *Environ. Sci. Technol*. 47 (21):12566–74. doi: 10.1021/es402265y.

Lim, Y. B., and P. J. Ziemann. 2009. Effects of molecular structure on aerosol yields from OH radical-initiated reactions of linear, branched, and cyclic alkanes in the presence of NOx. *Environ. Sci. Technol*. 43 (7):2328–34. doi: 10.1021/es803389s.

Lopez-Hilfiker, F. D., C. Mohr, M. Ehn, F. Rubach, E. Kleist, J. Wildt, T. F. Mentel, A. Lutz, M. Hallquist, D. Worsnop, et al. 2014. A novel method for online analysis of gas and particle composition: Description and evaluation of a filter inlet for gases and AEROsols (FIGAERO). *Atmos. Meas. Technol*. 7 (4):983–1001. doi: 10.5194/amt-7-983-2014.

Maricq, M., R. Chase, N. Xu, and P. Laing. 2002. The effects of the catalytic converter and fuel sulphur level on motor vehicle particulate matter emissions: Light duty diesel vehicles. *Environ. Sci. Technol*. 36 (2):283–89. doi: 10.1021/es010962l.

Maricq, M. M. 2007. Chemical characterization of particulate emissions from diesel engines: A review. *J. Aerosol Sci*. 38 (11):1079–118.

Norman, A. A., Y. Kado, R. A. Okamoto, B. A. Holmen, P. A. Kuzmicky, R. Kobayashi, and K. E. Stiglitz. 2002. Diesel and CNG heavy-duty transit bus emissions over

multiple driving schedules: Regulated pollutants and project overview, SAE Technical Paper Series. 2002-01-1722. doi:10.4271/2002-01-1722.

Olson, C. N., M. M. Galloway, G. Yu, C. J. Hedman, M. R. Lockett, T. Yoon, E. A. Stone, L. M. Smith, and F. N. Keutsch. 2011. Hydroxycarboxylic acid-derived organosulphates: Synthesis, stability, and quantification in ambient aerosol. *Environ. Sci. Technol.* 45 (15):6468–74. doi: 10.1021/es201039p.

Ots, R., D. E. Young, M. Vieno, L. Xu, R. E. Dunmore, J. D. Allan, H. Coe, L. R. Williams, S. C. Herndon, N. L. Ng, et al. 2016. Simulating secondary organic aerosol from missing diesel-related intermediate-volatility organic compound emissions during the clean air for London (ClearfLo) campaign. *Atmos. Chem. Phys. Discuss.* 16 (10):6453–73. doi:10.5194/acp-16-6453-2016.

Platt, S. M., I. E. Haddad, S. M. Pieber, A. A. Zardini, R. Suarez-Bertoa, M. Clairotte, K. R. Daellenbach, R.-J. Huang, J. G. Slowi, S. Hellebust, et al. 2017. Gasoline cars produce more carbonaceous particulate matter than modern filter-equipped diesel cars. *Sci. Rep.* 7:4926.

Pieber, S. M., N. K. Kumar, F. Klein, P. Comte, D. Bhattu, J. Dommen, E. A. Bruns, D. Kılıç, I. El Haddad, A. Keller, et al. 2018. Gas-phase composition and secondary organic aerosol formation from standard and particle filter-retrofitted gasoline direct injection vehicles investigated in a batch and flow reactor. *Atmos. Chem. Phys.* 18 (13):9929–54. doi: 10.5194/acp-18-9929-2018.

Pirjola, L., P. Karjalainen, J. Heikkila, S. Saari, T. Tzamkiozis, L. Ntziachristos, K. Kulmala, J. Keskinen, and T. Ronkko. 2015. Effects of fresh lubricant oils on particle emissions emitted by a modern gasoline direct injection passenger car. *Environ. Sci. Technol.* 49 (6): 3644–52. doi:10.1021/es505109u.

Pirjola, L., A. Dittrich, J. V. Niemi, S. Saarikoski, H. Timonen, H. Kuuluvainen, A. Järvinen, A. Kousa, R. Hillamo. 2016. Physical and chemical characterization of real-world particle number and mass emissions from city buses in Finland. *Environ. Sci. Technol.* 50 (1):294–304. doi: 10.1021/es505109u. doi: 10.1021/acs.est.5b0410549(6): 3644-52.

Pope, C. A., and D. W. Dockery. 2006. Health effects of fine particulate air pollution: Lines that connect. *J. Air Waste Manage. Assoc.* 56 (6):709–42. doi: 10.1080/10473289.2006.10464485.

Roberts, J. M., P. Veres, C. Warneke, J. A. Neuman, R. A. Washenfelder, S. S. Brown, M. Baasandorj, J. B. Burkholder, I. R. Burling, T. J. Johnson, et al. 2010. Measurement of HONO, HNCO, and other inorganic acids by negative-ion proton-transfer chemical-ionization mass spectrometry (NI-PT-CIMS): Application to biomass burning emissions. *Atmos. Meas. Technol.* 3 (4): 981–90. doi: 10.5194/amt-3-981-2010.

Robinson, A. L., N. M. Donahue, M. K. Shrivastava, E. A. Weitkamp, A. M. Sage, A. P. Grieshop, T. E. Lane, J. R. Pierce, S. N. Pandis. 2007. Rethinking organic aerosols: semivolatile emissions and photochemical aging. *Science* 315 (5816):1259–62. doi: 10.1126/science.1133061.

Robinson, M. A., M. R. Olson, Z. G. Liu, and J. J. Schauer. 2015. The effects of emission control strategies on light absorbing carbon emissions from a modern heavy-duty diesel engine. *J. Air Waste Manage.* 65 (6):759–66. doi: 10.1080/10962247.2015.1005850.

Saarkoski, S., H. Timonen, S. Carbone, H. Kuuluvainen, J. V. Niemi, A. Jousa, T. Rönkkö, D. Worsnop, R. Hilamo, and L. Pirjola. 2017. Investigating, the chemical species in submicron particles emitted by city buses. *Aerosol Sci. Technol* 51 (3): 317–29. doi: 10.1080/02786826.2016.1261992.

Smith, J. N., M. J. Dunn, T. M. VanReken, K. Iida, M. R. Stolzenburg, P. H. McMurry, and L. G. Huey. 2008. Chemical composition of atmospheric nanoparticles formed from nucleation in tecamac, Mexico: Evidence for an important role for organic species in nanoparticle growth. *Geophys. Res. Lett.* 35:L04808. doi: 10.1029/2007GL032523.

Tkacik, D. S., A. T. Lambe, S. Jathar, X. Li, A. A. Presto, Y. Zhao, D. Blake, S. Meinardi, J. T. Jayne, P. L. Croteau, et al. 2014. Secondary organic aerosol formation from in-use motor vehicle emissions using a potential aerosol mass reactor. *Environ. Sci. Technol.* 48 (19):11235–242. doi: 10.1021/es502239v.

Ullman, T. L., L. R. Smith, J. W. Anthony, W. J. Slodowske, B. Trestrail, A. L. Cook, W. B. Bunn, C. A. Lapin, K. J. Wright, and C. R. Clark. 2003. Comparison of exhaust emissions, including toxic air contaminants, from school buses in compressed natural gas, low emitting diesel, and conventional diesel engine configurations, SAE Technical Paper Series. 2003-01-1381. doi:10.4271/2003-01-1381.

United Nations, Department of Economic and Social Affairs, Population Division. 2018. World Urbanization Prospects: The 2018 Revision, Online Edition. https://esa.un.org/unpd/wup/Publications.

Usmanov, R. A., S. V. Mazanov, A. R. Gabitova, L. Miftakhova, F. M. khGumerov, R. Z. Musin, and I. M. Abdulagatov. 2015. The effect of fatty acid ethyl esters concentration on the kinematic viscosity of biodiesel fuel. *J. Chem. Eng. Data* 60 (11):3404–13. doi: 10.1021/acs.jced5b00683.

Volkamer, R., U. Platt, and K. Wirtz. 2001. Primary and secondary glyoxal formation from aromatics: Experimental evidence for the bicycloalkyl – radical pathway from benzene, toluene, and p-xylene. *J. Phys. Chem. A* 105 (33):7865–74. doi: 10.1021/jp010152w.

Watne, Å. K., M. Psichoudaki, E. Ljungström, M. Le Breton, M. Hallquist, M. Jerksjö, H. Fallgren, S. Jutterström, and Å. M. Hallquist. 2018. Fresh and oxidized emissions from in-use transit buses running on diesel, biodiesel, and CNG. *Environ. Sci. Technol.* 52 (14):7720–28.

Wentzell, J. J. B., J. Liggio, S.-M. Li, A. Vlasenko, R. Staebler, G. Lu, M.-J. Poitras, T. Chan, and J. R. Brook. 2013. Measurements of gas phase acids in diesel exhaust: A relevant source of HNCO? *Environ. Sci. Technol.* 47 (14):7663–71.

Worton, D. R., G. Isaacman, D. R. Gentner, T. R. Dallmann, A. W. H. Chan, C. Ruehl, T. W. Kirchstetter, K. R. Wilson, R. A. Harley, and A. H. Goldstein. 2014. Lubricating oil dominates primary organic aerosol emissions from motor vehicles. *Environ. Sci. Technol.* 48 (7): 3698–706. doi: 10.1021/es405375j.